Identification of Unique Fragmentation Patterns of Fentanyl Analog Protomers using Structures for Lossless Ion Manipulations Ion Mobility-Orbitrap Mass Spectrometry

Adam L. Hollerbach^{1*}, Yehia M. Ibrahim¹, Vivian S. Lin¹, Katherine J. Schultz¹, Adam P. Huntley¹, P. B. Armentrout², Thomas O. Metz¹, Robert G. Ewing³

Corresponding Author

* adam.hollerbach@pnnl.gov

¹ Biological Sciences Division, Pacific Northwest National Laboratory, Richland, Washington, 99354, United States

² Department of Chemistry, University of Utah, Salt Lake City, Utah, 84112, United States

³ Nuclear, Chemistry & Biology Division, Pacific Northwest National Laboratory, Richland, Washington, 99354, United States

Abstract

The opioid crisis in the United States is being fueled by the rapid emergence of new fentanyl analogs and precursors that can elude traditional library-based screening methods, which require data from known reference compounds. Since reference compounds are unavailable for new fentanyl analogs, we examined if fentanyls (fentanyl + fentanyl analogs) could be identified in a reference-free manner using a combination of electrospray ionization (ESI), high-resolution ion mobility (IM) spectrometry, high-resolution mass spectrometry (MS), and higher-energy collision-induced dissociation (MS/MS). We analyzed a mixture containing nine fentanyls and W-15 (a structurally similar molecule) and found that the protonated forms of all fentanyls uniquely exhibited two baseline separated IM distributions that produced different MS/MS patterns. Upon fragmentation, both IM distributions of all fentanyls produced two high intensity fragments resulting from amine site cleavages. The higher mobility distributions of all fentanyls also produced several low intensity fragments, but surprisingly, these same fragments exhibited much greater intensities in the lower mobility distributions. This observation demonstrates that many fragments of fentanyls predominantly originate from one of two different gas-phase structures (suggestive of protomers). Furthermore, increasing the water concentration in the ESI solution increased the intensity of the lower mobility distribution relative to the higher mobility distribution, which further supports that fentanyls exist as two gas-phase protomers. Our new observations on the IM and MS/MS properties of fentanyls can be exploited to positively identify them as fentanyls without requiring reference libraries and will hopefully assist first responders and law enforcement in combating new and emerging fentanyls.

Keywords: analog, CID, electrospray ionization, fentanyl, fingerprint, gas-phase, high resolution, ion mobility, mass accuracy, mass spectrometry, Orbitrap, reference-free, SLIM, traveling wave

Introduction

Fentanyl and fentanyl analogs (collectively termed fentanyls) have become leading causes of opioid-related deaths in the United States.¹ Fentanyl is a synthetic opioid originally developed as a pain reliever / anesthetic that binds the mu-opioid receptor (MOR) 4 to 430 times more strongly than heroin and morphine.²⁻⁸ The fentanyl backbone contains many chemical sites that can be easily and inexpensively modified to create fentanyl analogs.⁹ Some fentanyl analogs, like carfentanil, can exhibit more than 100x the potency of fentanyl itself (~10,000x the potency of morphine),³ thus making them very dangerous. Unfortunately, once fentanyl analogs are identified and incorporated into screening libraries, new fentanyl analogs begin to emerge that many library-based screening approaches will not detect.¹ Sensitive and robust techniques that do not rely on library searches are therefore needed so that new fentanyl analogs can be detected in real-time with high confidence.

Mass spectrometry (MS) is widely used for screening and identifying novel fentanyl analogs due to its high chemical specificity, high sensitivity, and ability to be coupled to complimentary analytical techniques.¹⁰ Fentanyl is readily analyzed by MS because its backbone possesses a high proton affinity (e.g., piperidine nitrogen = 1058.9-1069.7 kJ/mol). ^{11,12} This means fentanyl and fentanyl analogs are readily ionized by soft ionization techniques like electrospray ionization (ESI) and atmospheric pressure chemical ionization (APCI). Further, fentanyls are likely to outcompete interferent compounds for the electrical charge, which facilitates their detection at very low concentrations using MS (e.g., low femtogram quantities). 11 The current paradigm to screen for fentanyls with MS involves comparing measurements to reference libraries containing mass measurements and fragmentation spectra obtained through analysis of reference compounds. 1,13 Gas chromatography (GC) coupled with electron ionization (EI) and MS was the first MS-based approach for fentanyl identification and provides highly reproducible fragmentation patterns with scoring metrics to determine whether a compound matches a known fentanyl fragmentation pattern (number of fragments, m/z, and intensity). Some GC-MS methods can even differentiate some positional isomers of fentanyls (i.e., same functional group at a different position) based on the relative intensities of shared fragment ions.¹⁴ Other MS-based methods involve measuring a fentanyl analog's exact mass using high-resolution MS (e.g., Orbitrap) and filtering based on mass defect (the difference between measured exact mass and

theoretical mass). 15,16 Similarly, the combination of high-resolution MS, fragmentation, and liquid chromatography (LC) is the current gold standard method for fentanyl screening and identification. 10 The main disadvantage of library-based compound identification methods is that they can only be used to identify known compounds, and this prevents confident identification of new compounds, such as emerging fentanyl analogs.

Many positional isomers of fentanyls often cannot be distinguished by fragmentation alone, although multistage mass spectrometry (MSⁿ) experiments have shown potential in this area.¹⁷ Therefore, researchers have begun analyzing mixtures of fentanyl and fentanyl analogs with ion mobility (IM) spectrometry, which separates gas-phase ions based on their size (rotationally averaged collision cross section (CCS)) and electrical charge.¹⁸⁻²⁰ Zaknoun et al. used a portable commercial drift tube (DT) IM spectrometer and atmospheric pressure chemical ionization (APCI) ionization to detect six novel fentanyl analogs in samples seized by law enforcement.²⁰ Interestingly, each of the six fentanyl analogs exhibited two IM separable distributions with different intensities. The authors proposed that the presence of two distinct IM distributions could be used to differentiate fentanyl analogs from non-fentanyl compounds in complex samples. This hypothesis was later supported by Butler and Baker who analyzed a mixture of thirty-three opioids using electrospray ionization (ESI) and DT-IM. They demonstrated that fentanyl was the only opioid to exhibit two distinct IM distributions with near equal intensities.¹⁹

Butler and Baker rationalized that the two IM distributions were either gas-phase conformations or protomers. The same claims were later echoed by Aderorho and Chouinard while studying the effects of using metal cation adducts to achieve better IM separation between structurally similar fentanyl analogs.¹⁸ While these previous hypotheses were based on experimental observations, Lau et al. addressed this question by using density functional theory (DFT) to theoretically explore the fragmentation pathways of three possible fentanyl protomers ((1) amide oxygen, (2) amide nitrogen, (3) piperidine nitrogen; see Supporting Information Figure S1 for chemical structure of fentanyl with labeled protonation sites).¹² The three protomers required different enthalpies and Gibbs energies to produce fragments of the same m/z (potentially isomers and/or tautomers), which suggests that certain fragments of fentanyls are produced from different protomers. Although no experimental data appears to exist to support that fentanyls

exhibit gas-phase protomers, other experimental and simulation studies performed on benzocaine and para-amino benzoic acid protomers indicate that this conclusion holds.^{21,22}

Most studies involving IM measurements of fentanyls used drift tubes (DT-IM). These systems typically provide up to ~100 resolving power, which is insufficient to resolve structurally similar fentanyls, although some DT-IM systems can partially resolve the bimodal IM distributions of individual fentanyls. However, IM separations performed with structures for lossless ion manipulations (SLIM) can routinely achieve 200 resolving power of protonated ions (e.g., peptides), making it potentially useful for fentanyl analysis.²³ The high resolving powers achieved in SLIM are accomplished by separating ions over long serpentine path lengths (>10 m) that can be even further extended in systems with ion cycling (> 1000 m demonstrated) or multilevel capabilities (up to 43 m demonstrated).²⁴ Recently, we coupled SLIM with Orbitrap MS and demonstrated simultaneous acquisition of IM separations over 11 meters, mass analysis at the highest mass resolution setting (Q-Exactive Plus Orbitrap = 140k), and higher-energy collision-induced dissociation (HCD). This multimodal high-resolution approach was envisioned to be well-suited for analyzing fentanyl analogs because IM can separate positional isomers and provide diagnostic markers in the form of two IM distributions, exact mass measurements can provide mass defect filtering, and fragmentation can provide characteristic structural motifs.

Here we showcase the first measurements of fentanyl analogs using a combination of ESI, high resolution IM, and high-resolution MS/MS performed with a dual-gated SLIM-Orbitrap instrument.²⁵ Our experiments reveal that fentanyl and fentanyl analogs indeed exhibit bimodal IM distributions with strikingly different fragmentation patterns that supports the existence of two gas-phase protomers. We use the experimental data as evidence to propose an additional criterion for fingerprinting fentanyl analogs based on high-resolution IM-MS/MS data with the goal of moving fentanyl analysis away from library-based approaches and towards reference-free chemical identification methodologies.

Experimental Details

Chemicals

Fentanyl, eight fentanyl analogs, and W-15 (a structurally similar molecule) were purchased from Cayman Chemical (Ann Arbor, MI, USA) as 100 µg/mL or 1 mg/mL methanolic

solutions. The eight fentanyl analogs were: (1) 4'-methyl acetyl fentanyl- d_5 , (2) β -methyl fentanyl, (3) ortho-fluoroisobutyryl fentanyl, (4) (\pm)-cis-3-methyl butyryl fentanyl, (5) furanyl fentanyl 3-furancarboxamide, (6) para-chloroisobutyryl fentanyl, (7) cyclohexyl fentanyl, and (8) 2,2,3,3-tetramethyl-cyclopropyl fentanyl. The chemical structures of fentanyl, the eight fentanyl analogs, and W-15 are provided in the Supporting Information for easier referencing (Figure S2). All fentanyl analogs were purchased as Drug Enforcement Agency (DEA) exempt preparations. Five tetraalkylammonium salts (TAAs: butyl-, pentyl-, hexyl-, heptyl-, octyl- denoted as C4 – C8, respectively) were purchased from Sigma-Aldrich (St. Louis, MO, USA) and were used as internal CCS calibrants. Mixtures of fentanyl, fentanyl analogs, and W-15 were prepared at 100 nM or 1 μ M equimolar concentration in methanol or 1:1 methanol:water. The TAAs were prepared at 100 nM equimolar concentration. The two mixtures analyzed in this study both contained fifteen compounds.

Instrumentation

All IM-MS/MS experiments were performed using a previously described dual-gated SLIM-Orbitrap platform in positive ion mode.²⁵ Briefly, the SLIM-Orbitrap is composed of comprises an 11 m path length SLIM coupled to a Q-Exactive Plus Orbitrap MS (Thermo-Fisher, Waltham, MA, USA). The SLIM and Orbitrap are coupled together using the conventional dual-gated scanning technique.²⁶ The SLIM-Orbitrap is able to simultaneously perform IM separations over 11 meters, mass analysis using the Orbitrap's highest mass resolution setting (140k), and higher-energy collision-induced dissociation (HCD). Nitrogen was used as the buffer gas for the SLIM (2.2-2.3 Torr) and the Orbitrap HCD cell (pressure automatically adjusted based on instrument conditions). All HCD experiments were performed using non-normalized collision energies (CE). The Orbitrap was calibrated using Pierce LTQ Velos ESI positive ion calibration solution (Thermo-Fisher, Waltham, MA, USA) immediately prior to all experiments. All solutions were directly infused using an HF-etched fused-silica nanoelectrospray emitter (20 µm o.d.) and a syringe pump (Harvard Apparatus, Holliston, MA, USA).²⁷

Signal processing and data analysis

Data were acquired as .RAW files by the Orbitrap, converted to .mzXML files using the 'MSConvert' tool from ProteoWizard,²⁸ and then imported into Matlab (Mathworks, Natick, MA, USA) for data processing and plotting. All extracted IM spectra were taken over *m/z* windows of

±0.005 amu. Mass defects (Δmmu) were calculated using XCalibur software. Chemical structures were drawn using the Chemical Sketch Tool web app from the RSCB Protein DataBank (https://www.rcsb.org/chemical-sketch).

Results and Discussion

High-resolution IM-MS of fentanyl and fentanyl analogs

Figure 1A shows a reconstructed SLIM separation acquired with high resolution Orbitrap mass analysis of the fifteen-component mixture of fentanyl, fentanyl analogs, W-15, and TAAs. Eighteen IM distributions with strong intensity were observed, and most of the IM distributions exhibited arrival times between 190 and 310 ms. A snapshot of the raw IM spectrum and MS acquired using the vendor processing software XCalibur is provided in the Supporting Information (Figure S3). Note that the x-axis in Figure S3 is labeled as 'time' (typically retention time), but it actually corresponds to 'arrival time' (the conversion from 'retention time / scan number' to 'arrival time' is detailed in a previous study). Two sets of extracted IM spectra were generated to better visualize the constituents of the fentanyl mixture and to determine if overlapping IM distributions were isomers or different compounds. The first set of extracted IM spectra shows overlaid spectra of the five TAAs (Figure 1B). As can be seen, all five TAAs were readily distinguished and exhibited only one distribution per *m/z*. Additionally, the arrival times (and CCSs) of the five TAAs bracketed those of fentanyl and the fentanyl analogs, which is important for obtaining higher accuracy CCS values of analytes of interest in traveling wave-based IM instruments. 29

Next, IM spectra of the protonated monoisotopic masses of fentanyl, the eight fentanyl analogs, and W-15 were extracted (\pm 0.005 amu window) and are plotted in Figure 1C. Note that a narrower arrival time window is shown in this figure compared to Figure 1B to view the different distributions more easily. As can be seen, fentanyl, the eight fentanyl analogs, and W-15 possessed arrival times between 200 and 300 ms. Interestingly, these overlaid spectra showed two baseline separated distributions for fentanyl and all eight fentanyl analogs. The higher mobility distribution of each fentanyl was more intense than the lower mobility distribution by 3.9 to 7.7 times, with an average of 6.6 ± 1.4 times (mean \pm 1 standard deviation). Additionally, the average separation between the two IM distributions of fentanyl and each fentanyl analog was ~20.0 ms (range = 12.0 – 28.4 ms). Previous studies by at least two other research groups have shown that protonated

fentanyl and fentanyl analogs exhibit two distinct IM distributions. ^{19,20} In our study, the SLIM provided baseline separation between the two distributions, and the Orbitrap confirmed that each set of distributions possessed the same exact mass. Interestingly, W-15 (Figure 1C, purple trace, labeled 2a) only exhibited a single IM distribution. W-15 is not a fentanyl analog, but it does possess similar structural characteristics to fentanyl, such as an ethyl-benzene bonded to a piperidine ring nitrogen (see Supporting Information Figure S2). Regardless, the observation that fentanyl and all eight fentanyl analogs exhibited two IM distributions while a structurally similar compound only exhibited one distribution highlights the diagnostic utility of IM for differentiating fentanyl-containing mixtures from coexisting and interferent compounds.

An IM calibration plot was generated to calculate the ^{TW}CCS_{N2} of the fentanyl-related constituents and is shown in the Supporting Information along with a 95% confidence band (Figure S4). The CCS-based resolving power of each IM distribution was calculated using equation (1):

$$R_{p} = \frac{CCS}{\Delta CCS} \tag{1}$$

where CCS and Δ CCS are the peak center and full width at half maximum (fwhm), respectively, in the CCS domain. A summary of all the SLIM-Orbitrap measurements for the TAA cations, fentanyl, and fentanyl analogs is given in the Supporting Information in Table S1. The table includes the following information: (1) chemical name, (2) peak number assigned in Figure 1, (3) chemical formula, (4) exact mass measurements from the Orbitrap, (5) mass error relative to predicted molecular formula, (6) peak center from SLIM separation, (7) fwhm, (8) $^{TW}CCS_{N2}$ measurements from the SLIM, and (9) $^{TW}CCS_{N2}$ -based resolving power. Note that the table includes experimentally measured values for both IM distributions of fentanyl and the eight fentanyl analogs. The average Rp^{CCS} obtained for protonated fentanyl, fentanyl analogs, and W-15 was 222.

We also observed that smaller (and lighter) fentanyl analogs generally exhibited smaller $^{TW}CCS_{N2}$ differences between the two IM distributions whereas larger (and heavier) fentanyl analogs generally exhibited larger $^{TW}CCS_{N2}$ differences. Figure 2 shows a plot of the difference in $^{TW}CCS_{N2}$ between the higher and lower mobility distributions versus the $^{TW}CCS_{N2}$ of the higher mobility distributions of fentanyl and the eight fentanyl analogs. As can be seen, a $\Delta^{TW}CCS_{N2}$ of 3.85 Å² was obtained for 4'-methyl acetyl fentanyl-d₅, which was the smallest fentanyl analog

analyzed in this study (m/z 342.2592, CCS = 183.25 and 187.10 Å²). A larger $\Delta^{TW}CCS_{N2}$ of 8.39 Å² was obtained for 2,2,3,3-tetramethyl-cyclopropyl fentanyl, which was the largest fentanyl analyzed in this study (m/z 405.2905, CCS = 201.81 and 210.20 Å²). The Δ CCS between the two IM distributions of the other fentanyl analogs fell between these two end points in a roughly linear manner (Figure 2, red line), although β -methyl fentanyl (pink dot) and ortho-fluoroisobutyryl fentanyl (light purple dot) exhibited noticeably higher $\Delta^{TW}CCS_{N2}$ than the other fentanyl analogs. It seems logical to expect that the two IM distributions of a potential novel fentanyl analog would also exhibit greater or lesser separation based on their size.

We also observed that the higher mobility distributions of fentanyl (black trace, peak 2b) and 4'-methyl acetyl fentanyl-d₅ (green trace, peak 3) were separated with a resolution of 0.86 (see Figure 1). The resolution between the two distributions was calculated according to equation (2):

$$Resolution_{pp} = \frac{1.18 * (td_2 - td_1)}{fwhm_2 + fwhm_1}$$
 (2)

where td and fwhm are the center and full width at half-maximum of the IM distribution, respectively. This separation is notable because the fentanyl and 4'-methyl acetyl fentanyl-d₅ are positional isomers, and traditional DT-IM methods typically struggle to achieve clear separation of fentanyl analog isomers. However, an 11-meter SLIM separation provided near baseline resolution. The two main structural differences between fentanyl and 4'-methyl acetyl fentanyl-d₅ are: (1) five deuterations at the anilide aromatic ring (see Figure S1), and (2) a methyl shift from the amide R group to the para position in the ethyl-benzene ring. We expect that the shifting of a methyl group from one side of an ion to the other was the primary contributor to the separation, while the deuterations only provided a minor, if even noticeable, contribution to the separation. The latter claim is supported by previous studies that have found that ions possessing one to five isotopic labels (e.g., tandem mass tag (TMT) fragments) only possess slightly larger CCS compared to ions without the isotopic labels (less than 0.01 Å² difference).²³ Our choice to use the deuterated version of 4'-methyl acetyl fentanyl instead of the undeuterated version was to ensure it could be differentiated from all other coexisting chemicals (either with IM or MS). However, our results suggest that SLIM would provide separation between fentanyl and undeuterated 4'-methyl acetyl fentanyl. The main point is that SLIM can differentiate positional isomers of fentanyl that are not readily separated with other IM techniques.

We also observed that the lower mobility distributions of fentanyl and 4'-methyl acetyl fentanyl- d_5 largely overlapped (peaks 5a and 5b, $\Delta^{TW}CCS_{N2} = 0.15$ Å²), whereas the higher mobility distributions of each were nearly baseline separated (peaks 2b and 3, $\Delta^{TW}CCS_{N2} = 1.24$ Å²). This observation highlights the usefulness of having two distinct IM distributions to identify fentanyl analogs. As with this example, one set of IM distributions can be overlapped (i.e., the lower mobility distributions) and provide no clear differentiation while the other set of IM distributions (i.e., the higher mobility distributions) can be well separated and provide clear differentiation. It is likely that cyclic or multilevel SLIM separations would better resolve the lower mobility distributions of fentanyl and 4'-methyl acetyl fentanyl- d_5 . The other fentanyl analogs analyzed in this study exhibited some level of separation between both the higher and lower mobility distributions. However, the possibility that one set of IM distributions can overlap while the other set does not (e.g., the higher mobility distributions can overlap while the lower IM distributions do not) is something to consider when looking for novel fentanyl analogs.

Influence of water on IM distributions

Since our results showed that the lower mobility distributions of fentanyl and the eight fentanyl analogs exhibited much lower intensity than the higher mobility distributions, we wondered if there was a way to increase the signal intensity of the lower mobility distributions so that both distributions could be readily observed. Ensuring the presence of two high intensity distributions would aid in screening for novel fentanyl analogs by ensuring that the low intensity lower mobility distributions would not be missed and would provide fundamental insights into why fentanyl analogs yield two IM separable distributions.

Surprisingly, we found that adding water to the ESI solvent greatly affected the ratio of IM distribution intensities. We repeated the same experiments (e.g., SLIM-Orbitrap acquisition parameters, analyte concentration) as above, only in this experiment we used a solvent consisting of 1:1 water:methanol, whereas the solvent in our initial experiment was pure methanol. Extracted IM spectra for the mixture of fentanyl and all eight fentanyl analogs in 1:1 methanol:water are shown in Figure 3. As can be seen, there was a large increase in the signal intensities of the lower mobility distributions for fentanyl and all eight fentanyl analogs. The effect of adding water to the ESI solvent was most pronounced for fentanyl (Figure 3A), (±)-cis-3-methyl butyryl fentanyl (Figure 3E), and 2,2,3,3-tetramethyl-cyclopropyl fentanyl (Figure 3I). The lower mobility

distributions for these three compounds exhibited higher intensities than the higher mobility distributions, which is the reverse of what was observed in pure methanol (where the higher mobility IM distribution exhibited higher intensity in methanol). A near 1:1 ratio was obtained for 4'-methyl acetyl fentanyl-d₅ (Figure 3B, green), β-methyl fentanyl (Figure 3C, pink), and cyclohexyl fentanyl (Figure 3H, orange). We also observed a less than 1:1 ratio of signal intensities for ortho-fluoroisobutyryl fentanyl (Figure 3D, light purple), furanyl fentanyl 3-furancarboxamide (Figure 3F, red), and para-chloroisobutyryl fentanyl (Figure 3G, light green). However, the intensities of the lower mobility distributions were markedly higher than those obtained in pure methanol solvent. Interestingly, an especially pronounced change in signal intensity was observed for 2,2,3,3-tetramethyl-cyclopropyl (Figure 3I) where the ratio of IM distribution intensities changed from 6.7:1 in methanol to 1:7.4 in 1:1 water:methanol. The direct comparison between solvents is shown in Figure 3J. This set of experiments demonstrated that using some amount of water during the ionization process (e.g., in the ESI solvent or humidity for APCI) is desirable to ensure that both IM distributions of fentanyl analogs can be more readily observed compared to using only methanol as the solvent.

The availability of water during ionization may be the reason that Butler and Baker observed near equal intensities for the two IM distributions of fentanyl, ¹⁹ while Zaknoun observed that the higher mobility distributions for six fentanyl analogs exhibited much greater intensities than the lower mobility distributions. ²⁰ While the two research groups used different ionization sources (ESI vs APCI), we postulate that the type of soft ionization source does not contribute as much as the availability of water contributes to the signal intensities of the two IM distributions. Humidity should largely dictate the amount of water available for APCI experiments, while water in solution should be the largest contributor to ESI. Additional experiments using APCI and different humidities are needed to confirm whether the presence of water definitively affects the intensity ratios of the two IM distributions of each fentanyl analog.

An intriguing question that arises from this solvent study is why using more water in the ESI solvent causes the ratio of the higher and lower mobility distributions of all fentanyl analogs to change. It is known that varying the water composition in an ESI solvent changes the intensities of observable gas-phase protomers of other drugs, such as benzocaine.²¹ In fact, Warnke et al. showed that higher water composition in the ESI solvent caused the bimodal IM distribution of

benzocaine (caused by two protomers) to shift towards the higher mobility distribution, while lower water concentration shifts the bimodal distribution towards the lower mobility distribution. These results are interesting to compare to our study because we observed the opposite trend for fentanyl and fentanyl analogs; i.e., we observed that higher water concentration causes the bimodal IM distributions to shift towards the lower mobility distribution, while lower water concentration shifts the bimodal distribution more towards the higher mobility distribution. Of course, benzocaine and fentanyl possess very different chemical structures, but our solvent study strongly suggests that fentanyl and fentanyl analogs exhibit two protomers, as opposed to other gas-phase conformational changes.

CID of individual IM distributions of fentanyl analogs

To further understand the composition of the two IM distributions for fentanyl and the eight fentanyl analogs, we performed higher-energy collision-induced dissociation (HCD) on each isolated IM distribution. Since the SLIM provided baseline separation between both distributions of a given m/z, we were able to confidently perform fragmentation on each IM distribution without being concerned that fragments from the other distribution would obscure the results. We performed two isolation steps prior to performing fragmentation to ensure that each distribution was isolated from the other IM distribution as well as from all other ions in the mixture of fentanyl analogs. First, we performed an IM filtering step using the second ion gate of the dual-gated SLIM. Each IM distribution was readily selected without any overlap from the other IM distribution since the SLIM provided baseline separation between each set of distributions. Second, a mass filtering step was performed using the Orbitrap's quadrupole mass filter (QMS). The mass isolation window of the QMS was centered on the exact mass of each ion and the narrowest possible mass isolation window (± 0.2 amu) was used. Ions were then sent to the HCD cell and higher-energy fragmentation using three different non-normalized collision energies (20, 25, 30) was performed. After fragmentation, ions were sent to the Orbitrap mass analyzer for high-resolution mass analysis (mass resolution setting = 140k).

Figure 4A shows the mass-selected IM spectrum of fentanyl acquired using the SLIM-Orbitrap, and Figure 4B and Figure 4C show fragmentation spectra of the higher and lower IM distributions of fentanyl (collision energy = 30). We note that we had to increase the concentration of fentanyl, all eight fentanyl analogs, and W-15 to 1 μ M equimolar concentration (in methanol)

to obtain sufficient ion intensities for fragmentation. The TAAs remained at 100 nM concentration. Figure 4B shows that the highest intensity fragment ions of the higher mobility distribution of fentanyl were m/z 188 (base peak) and m/z 105 (~39% intensity of base peak). These fragments were assigned manually and represent bond cleavages at the amide and piperidine nitrogens (m/z 188 and 105, respectively; see Figure S1). Other low-intensity fragment ions (<5% base peak intensity) were present, including m/z 132, 134, 146, and 216. The precursor ion (nominal m/z 337) also exhibited low intensity when using 30 collision energy, suggesting most of it was fragmented. The fragmentation spectrum of the lower mobility distribution of fentanyl (Figure 4C) was strikingly different than that of the higher mobility distribution. While m/z 188 was the highest intensity fragment in the spectrum in the higher mobility distribution, the same fragment ion exhibited a much lower relative intensity in the spectrum from the lower mobility distribution (~34% intensity of base peak). Instead, the highest intensity fragment ions were m/z 105 (base peak), 132, 134, and 216, which exhibited low abundances in the higher mobility distribution. These results indicate that the gas-phase structure of protonated fentanyl plays an important role in its fragmentation pathways.

Additionally, the precursor ion exhibited a higher relative intensity compared to the base peak than it did in the fragmentation spectrum from the higher mobility distribution (~34% vs ~7%). These data were acquired over >50 scans to ensure data averaging was not the contributor to the difference. To further validate that this finding was real, we performed the same experiments using two lower collision energies (20, 25). Fragmentation spectra of the two IM distributions of fentanyl using 20 and 25 collision energies are given in the Supporting Information (Figure S5). Even when lower collision energies were used, the higher mobility distribution still resulted in mostly fragment ions associated with amine bond cleavages, and the lower mobility distribution gave other fragment ions and a higher precursor ion intensity.

We also averaged the two IM distributions of fentanyl together and plotted the resulting MS/MS spectrum in Figure 4D for other researchers who perform CID on fentanyl analogs using different MS or IM-MS hybrid systems to compare to. However, we emphasize that the SLIM-Orbitrap shows that the fragment ions observed in a typical CID spectrum of fentanyl are actually produced from two distinct IM distributions. A bar plot was also generated to show the percentage each IM distribution contributes to the total fragment and precursor ion intensities in the composite

MS/MS spectrum (Figure 4E). This plot clearly shows that most of the fragment ions of fentanyl predominantly originate from one of the two IM distributions. To the best of our knowledge, this is the first demonstration of this phenomenon for fentanyl.

Interestingly, we also found that fentanyl was not the only compound whose two IM distributions exhibited different fragmentation patterns. In fact, the two IM distributions of all eight fentanyl analogs examined in this study exhibited different fragmentation patterns. These differences included the same three findings as observed for fentanyl: (1) the higher mobility distribution mostly exhibiting high intensity fragment ions associated with amine bond cleavages, (2) the lower mobility distribution exhibiting fragments corresponding to amine bond cleavages and other high intensity fragments, and (3) the lower mobility distribution exhibiting a higher precursor ion intensity at a given collision energy. The results of mobility and mass filtered fragmentation spectra of both IM distributions for all eight fentanyl analogs at 20, 25, and 30 collision energy are given in the Supporting Information (Figure S6 – Figure S13). We also included averaged fragmentation spectra of the two IM distributions for each fentanyl analog and bar plots showing the percentage each IM distribution contributions to fragment and precursor ion intensities in the composite MS/MS spectrum. These results demonstrate an additional criterion that potential new fentanyl analogs must meet to be considered true fentanyl analogs and not a different compound class. Mass-selected IM and MS/MS spectra for W-15 were also generated and are provided in the Supporting Information (Figure S14).

Since our results showed that the two IM distributions of fentanyl analogs fragment differently, we wondered whether the fragments from each distribution possess the same chemical structure or if they are isomers. Wichitnithad and coworkers surmised that the fragment ion from fentanyl with m/z 188 is actually two different isomers.³⁰ They proposed different fragmentation mechanisms complete with structures for comparison. A logical next step to decipher why two IM distributions exist, and why they exhibit different fragmentation patterns, is to perform a conformational search of protonated fentanyl followed by a DFT optimization. Interestingly, two studies have already explored using conformational searches and DFT optimizations to obtain energetically favorable gas-phase structures of protonated fentanyl, but for different reasons. In one study, Lau et al. investigated which of the three protonation sites in fentanyl was the most energetically favorable and used the information to propose fragmentation pathways and

products.¹² They found that protonating the piperidine nitrogen was the most energetically favorable and proposed an extended structure. They also found that protonating at the carbonyl oxygen and the amide nitrogen were both energetically disfavored, and doing so resulted in extended structures. In the other study, Denis et al. also found that protonating the piperidine nitrogen of fentanyl resulted in the most energetically favorable structure, and they then used this information to calculate fentanyl's proton affinity and gas-phase basicity.¹¹ However, they found that the most energetically optimized conformation of fentanyl showed the benzyl ring tilting towards the hydrogen bridge that was formed between the carbonyl oxygen and piperidine nitrogen. Performing DFT calculations using the new knowledge from this study would provide more insight into whether the two IM distributions of fentanyl and fentanyl analogs produce isobaric fragments, and whether the two IM distributions that yield these fragments are in fact protomers as the evidence in this study seems to suggest.

Conclusions

A SLIM-Orbitrap was used to demonstrate that fentanyl and eight fentanyl analogs all exhibit two baseline separable IM distributions that yield different fragmentation patterns, precursor ion stabilities, and relative intensities that depend on the concentration of water in solution. This study shows that fentanyl analogs exhibit unique fragmentation-based chemical signatures that can be used to help differentiate potentially new fentanyl analogs from other compounds. Additionally, our study on the effects of water concentration on IM peak intensity can help ensure that researchers will observe two IM distributions, which can then be fragmented. Having the additional metric that potential fentanyl analogs must exhibit two IM distributions that fragment differently may help in finding new fentanyl analogs in real-time without requiring a populated reference library, since it is unlikely that many compounds will exhibit this behavior.

Our studies strongly suggest that the two IM distributions of fentanyl and fentanyl analogs are protomers, but further modeling studies using quantum chemistry are needed to confirm this hypothesis. Additionally, these calculations would shed light into whether the chemical structures of the fragments produced by each IM distribution are identical or isobaric. Understanding both phenomena would be helpful in finding new fentanyl analogs and may potentially help identify

other unknown classes of illicit (or potentially illicit) opioids more rapidly. We hope such information will assist first responders and law enforcement in combating the opioid crisis.

Associated Content

Supporting Information

Chemical structure of fentanyl with labeled protonation sites and functional groups; Chemical structures of fentanyl, eight fentanyl analogs, and W-15; Snapshot of the raw IM spectrum and MS acquired with XCalibur software; IM calibration curve of reduced CCS vs arrival time; Table of SLIM-Orbitrap measurements on fentanyl mixture; Mass-selected IM and MS/MS spectra of fentanyl; Mass-selected IM and MS/MS spectra of 4'-methyl acetyl fentanyl-d₅; Mass-selected IM and MS/MS spectra of ortho-fluoroisobutyryl fentanyl; Mass-selected IM and MS/MS spectra of (±)-cis-3-methyl butyryl fentanyl; Mass-selected IM and MS/MS spectra of furanyl fentanyl 3-furancarboxamide; Mass-selected IM and MS/MS spectra of cyclohexyl fentanyl; Mass-selected IM and MS/MS spectra of 2,2,3,3-tetramethyl-cyclopropyl fentanyl; Mass-selected IM and MS/MS spectra of W-15

Author Information

Corresponding Author

Adam L. Hollerbach - Biological Sciences Division, Pacific Northwest National Laboratory, Richland, Washington 99354, United States

Authors

Yehia M. Ibrahim - Biological Sciences Division, Pacific Northwest National Laboratory, Richland, Washington 99354, United States

Vivian S. Lin - Biological Sciences Division, Pacific Northwest National Laboratory, Richland, Washington 99354, United States

Katherine J. Schultz - Biological Sciences Division, Pacific Northwest National Laboratory, Richland, Washington 99354, United States

Adam P. Huntley - Biological Sciences Division, Pacific Northwest National Laboratory, Richland, Washington, 99354, United States

P. B. Armentrout – Department of Chemistry, University of Utah, Salt Lake City, Utah, 84112, United States

Thomas O. Metz - Biological Sciences Division, Pacific Northwest National Laboratory, Richland, Washington, 99354, United States

Robert G. Ewing - Nuclear, Chemistry & Biology Division, Pacific Northwest National Laboratory, Richland, Washington, 99354, United States

Notes

All authors declare no competing financial interest.

This research was supported by the PNNL Laboratory Directed Research and Development Program and is a contribution of the m/q initiative. This project was performed in the Environmental Molecular Sciences Laboratory, a DOE Office of Biological and Environmental Research sponsored national scientific user facility located on the PNNL campus. Battelle operates PNNL for the DOE under contract DE-AC05-76RLO01830. The contribution of PBA was supported by the National Science Foundation, Grant CHE-2313553.

References

- (1) Armenian, P.; Vo, K. T.; Barr-Walker, J.; Lynch, K. L. Fentanyl, fentanyl analogs and novel synthetic opioids: A comprehensive review, *Neuropharmacology* **2018**, *134*, 121-132.
- (2) Janssen, P. A. J.; Van De Westeringh, C.; Jageneau, A. H. M.; Demoen, P. J. A.; Hermans, B. K. F.; Van Daele, G. H. P.; Schellekens, K. H. L.; Van Der Eycken, C. A. M.; Niemegeers, C. J. E. Chemistry and Pharmacology of CNS Depressants Related to 4-(4-Hydroxy-4-phenylpiperidino)butyrophenone Part I--Synthesis and screening data in mice, *Journal of Medicinal and Pharmaceutical Chemistry* **1959**, *1*, 281-297.
- (3) Comer, S. D.; Cahill, C. M. Fentanyl: Receptor pharmacology, abuse potential, and implications for treatment, *Neuroscience & Biobehavioral Reviews* **2019**, *106*, 49-57.
- (4) Terenius, L. Contribution of 'receptor' affinity to analgesic potency, *J. Pharm. Pharmacol.* **1974**, *26*, 146-148.
- (5) Kutter, E.; Herz, A.; Teschemacher, H. J.; Hess, R. Structure-activity correlations of morphinelike analgetics based on efficiencies following intravenous and intraventricular application, *J. Med. Chem.* **1970**, *13*, 801-805.
- (6) van den Hoogen, R. H. W. M.; Colpaert, F. C. Epidural and Subcutaneous Morphine, Meperidine (pethidine), Fentanyl and Sufentanil in the Rat: Analgesia and Other in vivo Pharmacologic Effects, *Anesthesiology* **1987**, *66*, 186-194.
- (7) Finch, J. S.; DeKornfeld, T. J. Clinical investigation of the analgesic potency and respiratory depressant activity of fentanyl, a new narcotic analgesic, *The Journal of Clinical Pharmacology and The Journal of New Drugs* **1967**, *7*, 46-51.
- (8) Vo, Q. N.; Mahinthichaichan, P.; Shen, J.; Ellis, C. R. How μ -opioid receptor recognizes fentanyl, *Nature Communications* **2021**, *12*, 984.
- (9) Vardanyan, R. S.; Hruby, V. J. Fentanyl-related compounds and derivatives: current status and future prospects for pharmaceutical applications, *Future Medicinal Chemistry* **2014**, *6*, 385-412.
- (10) Palmquist, K. B.; Truver, M. T.; Shoff, E. N.; Krotulski, A. J.; Swortwood, M. J. Review of analytical methods for screening and quantification of fentanyl analogs and novel synthetic opioids in biological specimens, *Journal of Forensic Sciences* **2023**, *n/a*.
- (11) Denis, E. H.; Bade, J. L.; Renslow, R. S.; Morrison, K. A.; Nims, M. K.; Govind, N.; Ewing, R. G. Proton Affinity Values of Fentanyl and Fentanyl Analogues Pertinent to Ambient Ionization and Detection, *J. Am. Soc. Mass. Spectrom.* **2022**, *33*, 482-490.
- (12) Lau, J. K.-C.; Romanov, V.; Lukow, S.; Hopkinson, A. C.; Verkerk, U. H. Collision-induced dissociation of protonated fentanyl: A DFT study, *Computational and Theoretical Chemistry* **2021**, *1196*, 113117.
- (13) Nan, Q.; Hejian, W.; Ping, X.; Baohua, S.; Junbo, Z.; Hongxiao, D.; Huosheng, Q.; Fenyun, S.; Yan, S. Investigation of Fragmentation Pathways of Fentanyl Analogues and Novel Synthetic Opioids by Electron Ionization High-Resolution Mass Spectrometry and Electrospray Ionization High-Resolution Tandem Mass Spectrometry, *J. Am. Soc. Mass. Spectrom.* **2020**, *31*, 277-291.
- (14) Mallette, J. R.; Casale, J. F.; Toske, S. G.; Hays, P. A. Characterization of (2R,4S)- and (2R,4R)-2-Methylfentanyl and their differentiation from cis- and trans-3-Methylfentanyl, *Forensic Chemistry* **2018**, *8*, 64-71.
- (15) Zhang, Y.; Halifax, J. C.; Tangsombatvisit, C.; Yun, C.; Pang, S.; Hooshfar, S.; Wu, A. H. B.; Lynch, K. L. Development and application of a High-Resolution mass spectrometry method for the detection of fentanyl analogs in urine and serum, *Journal of Mass Spectrometry and Advances in the Clinical Lab* **2022**, *26*, 1-6.

- (16) Swanson, D.; Stickle, D.; Evans-Nguyen, T. Analysis of unknown fentanyl analogs using high resolution mass spectrometry with mass defect filtering, *Int. J. Mass spectrom.* **2023**, *485*, 116992.
- (17) Davidson, J. T.; Sasiene, Z. J.; Jackson, G. P. The influence of chemical modifications on the fragmentation behavior of fentanyl and fentanyl-related compounds in electrospray ionization tandem mass spectrometry, *Drug Testing and Analysis* **2020**, *12*, 957-967.
- (18) Aderorho, R.; Chouinard, C. D. Improved separation of fentanyl isomers using metal cation adducts and high-resolution ion mobility-mass spectrometry, *Drug Testing and Analysis* **2023**, 1-11.
- (19) Butler, K. E.; Baker, E. S. A High-Throughput Ion Mobility Spectrometry–Mass Spectrometry Screening Method for Opioid Profiling, *J. Am. Soc. Mass. Spectrom.* **2022**, *33*, 1904-1913.
- (20) Zaknoun, H.; Binette, M.-J.; Tam, M. Analyzing fentanyl and fentanyl analogues by ion mobility spectrometry, *International Journal for Ion Mobility Spectrometry* **2019**, *22*, 1-10.
- (21) Warnke, S.; Seo, J.; Boschmans, J.; Sobott, F.; Scrivens, J. H.; Bleiholder, C.; Bowers, M. T.; Gewinner, S.; Schöllkopf, W.; Pagel, K.; von Helden, G. Protomers of Benzocaine: Solvent and Permittivity Dependence, *Journal of the American Chemical Society* **2015**, *137*, 4236-4242.
- (22) Demireva, M.; Armentrout, P. B. Relative Energetics of the Gas Phase Protomers of p-Aminobenzoic Acid and the Effect of Protonation Site on Fragmentation, *The Journal of Physical Chemistry A* **2021**, *125*, 2849-2865.
- (23) Wojcik, R.; Nagy, G.; Attah, I. K.; Webb, I. K.; Garimella, S. V. B.; Weitz, K. K.; Hollerbach, A.; Monroe, M. E.; Ligare, M. R.; Nielson, F. F.; Norheim, R. V.; Renslow, R. S.; Metz, T. O.; Ibrahim, Y. M.; Smith, R. D. SLIM Ultrahigh Resolution Ion Mobility Spectrometry Separations of Isotopologues and Isotopomers Reveal Mobility Shifts due to Mass Distribution Changes, *Anal. Chem.* **2019**, *91*, 11952-11962.
- (24) Hollerbach, A. L.; Li, A.; Prabhakaran, A.; Nagy, G.; Harrilal, C. P.; Conant, C. R.; Norheim, R. V.; Schimelfenig, C. E.; Anderson, G. A.; Garimella, S. V. B.; Smith, R. D.; Ibrahim, Y. M. Ultra-High-Resolution Ion Mobility Separations Over Extended Path Lengths and Mobility Ranges Achieved using a Multilevel Structures for Lossless Ion Manipulations Module, *Anal. Chem.* **2020**, *92*, 7972-7979.
- (25) Hollerbach, A. L.; Ibrahim, Y. M.; Meras, V.; Norheim, R. V.; Huntley, A. P.; Anderson, G. A.; Metz, T. O.; Ewing, R. G.; Smith, R. D. A Dual-Gated Structures for Lossless Ion Manipulations-Ion Mobility Orbitrap Mass Spectrometry Platform for Combined Ultra-High-Resolution Molecular Analysis, *Anal. Chem.* **2023**, *95*, 9531-9538.
- (26) Karasek, F. W.; Hill, H. H.; Kim, S. H. Plasma chromatography of heroin and cocaine with mass-identified mobility spectra, *J. Chromatogr. A* **1976**, *117*, 327-336.
- (27) Kelly, R. T.; Page, J. S.; Luo, Q.; Moore, R. J.; Orton, D. J.; Tang, K.; Smith, R. D. Chemically etched open tubular and monolithic emitters for nanoelectrospray ionization mass spectrometry, *Anal. Chem.* **2006**, *78*, 7796-7801.
- (28) Chambers, M. C.; Maclean, B.; Burke, R.; Amodei, D.; Ruderman, D. L.; Neumann, S.; Gatto, L.; Fischer, B.; Pratt, B.; Egertson, J.; Hoff, K.; Kessner, D.; Tasman, N.; Shulman, N.; Frewen, B.; Baker, T. A.; Brusniak, M.-Y.; Paulse, C.; Creasy, D.; Flashner, L., et al. A cross-platform toolkit for mass spectrometry and proteomics, *Nat. Biotechnol.* **2012**, *30*, 918-920.
- (29) May, J. C.; Leaptrot, K. L.; Rose, B. S.; Moser, K. L. W.; Deng, L.; Maxon, L.; DeBord, D.; McLean, J. A. Resolving Power and Collision Cross Section Measurement Accuracy of a Prototype High-Resolution Ion Mobility Platform Incorporating Structures for Lossless Ion Manipulation, *J. Am. Soc. Mass. Spectrom.* **2021**, *32*, 1126-1137.

(30) Wichitnithad, W.; McManus, T. J.; Callery, P. S. Identification of isobaric product ions in electrospray ionization mass spectra of fentanyl using multistage mass spectrometry and deuterium labeling, *Rapid Commun. Mass Spectrom.* **2010**, *24*, 2547-2553.

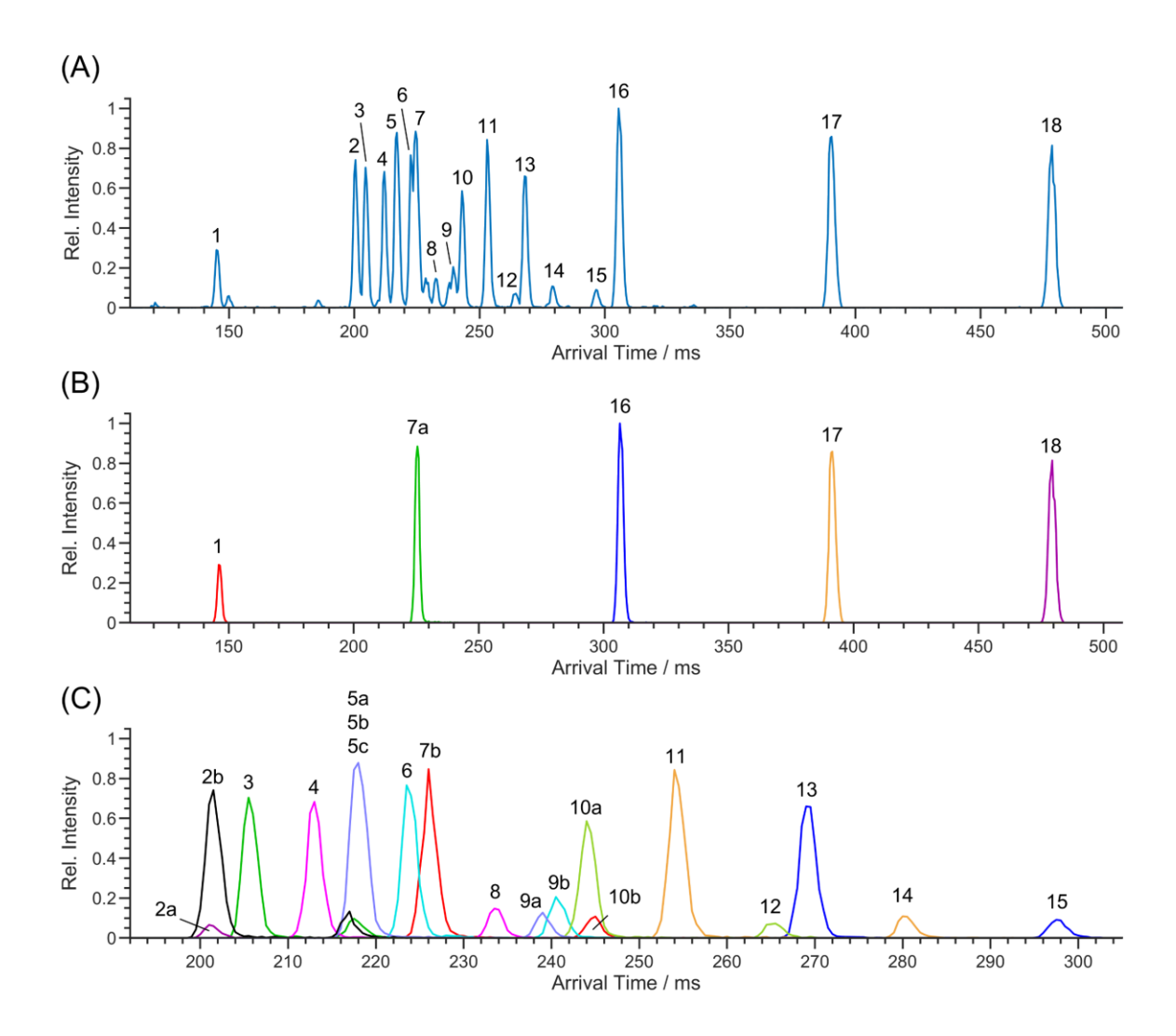


Figure 1: (A) SLIM separation (base peak intensity) of a mixture of fentanyl, eight fentanyl analogs, W-15, and five TAA cations. (B) Overlaid extracted IM spectra of TAA cations. Red = TAA_C4 (1), green = TAA_C5 (7a), blue = TAA_C6 (16), orange = TAA_C7 (17), purple = TAA_C8 (18). (C) Overlaid extracted IM spectra of fentanyl, fentanyl analogs, and W-15. Purple = W-15 (2a), black = fentanyl (2b, 5a), green = 4-methyl-acetyl fentanyl-d5 (3, 5b), pink = β-methyl fentanyl (4, 8), light purple = ortho-fluoroisobutyryl fentanyl (5c, 9a), light blue = (±)-cis-3-methyl butyryl fentanyl (6, 9b), red = furanyl fentanyl 3-furancarboxamide (7b, 10b), light green = para-chloroisobutyryl fentanyl (10a, 12), orange = cyclohexyl fentanyl (11,14), blue = 2,2,3,3-tetramethyl-cyclopropyl fentanyl. In-SLIM accumulation time = 20 ms. SLIM pressure = 2.28 Torr nitrogen. TW = 120 m/s at 17.5 V_{0-p}. Guard = 25 V. Dual-gate = 0.5 ms width, 0.5 ms / step. Scans per $\Delta t = 1$. Orbitrap mass resolution setting = 140k.

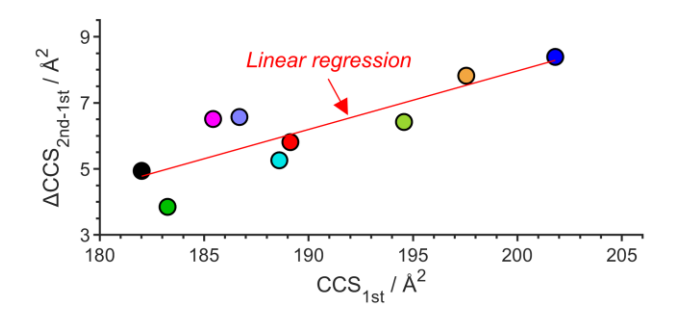


Figure 2: Plot of the CCS of the higher mobility distribution versus the difference in CCS between the lower and higher mobility distributions. Black = fentanyl, green = 4-methyl-acetyl fentanyl-d5, pink = β -methyl fentanyl, light purple = ortho-fluoroisobutyryl fentanyl, light blue = (\pm)-cis-3-methyl butyryl fentanyl, red = furanyl fentanyl 3-furancarboxamide, light green = parachloroisobutyryl fentanyl, orange = cyclohexyl fentanyl, blue = 2,2,3,3-tetramethyl-cyclopropyl fentanyl.

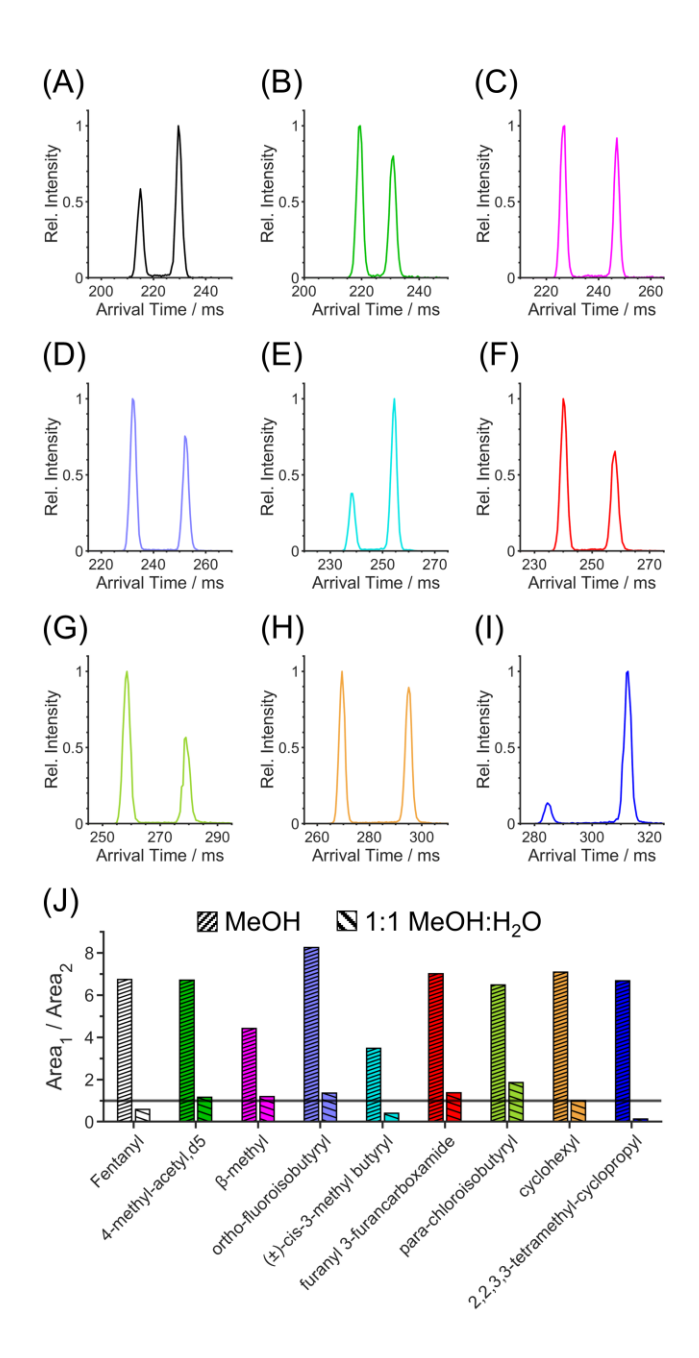


Figure 3: Extracted IM spectra of fentanyl and eight fentanyl analogs in 1:1 methanol:water. (A) fentanyl, (B) 4'-methyl acetyl fentanyl-d₅, (C) β-methyl fentanyl, (D) ortho-fluoroisobutyryl fentanyl, (E) (\pm)-cis-3-methyl butyryl fentanyl, (F) furanyl fentanyl 3-furancarboxamide, (G) parachloroisobutyryl fentanyl, (H) cyclohexyl fentanyl, (I) 2,2,3,3-tetramethyl-cyclopropyl fentanyl. (J) Comparison of IM peak areas for the two IM distributions of fentanyl and eight fentanyl analogs in pure methanol and 1:1 methanol:water. The solid horizontal line at y = 1 indicates when the areas of the two IM distributions for fentanyl and each fentanyl analog were equal.

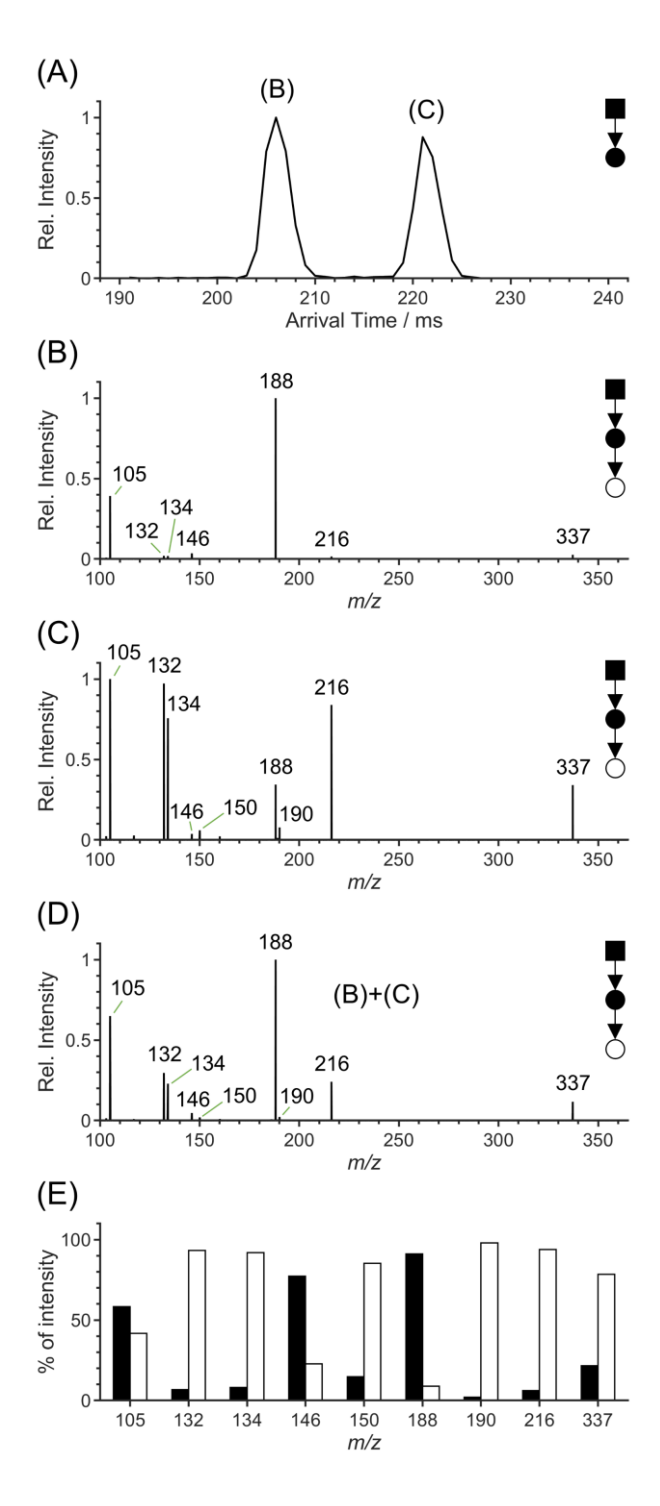


Figure 4: (A) SLIM IM spectrum of quadrupole mass isolated fentanyl (m/z 337.2 ± 0.2). (B,C) Averaged MS/MS spectra of the higher and lower mobility distributions, respectively. (D) Composite MS/MS spectrum of the higher and lower mobility distributions. (E) Bar plot showing the percentage each IM distribution contributions to fragment and parent ion intensities in the composite MS/MS spectrum. Black bars = higher mobility distribution. White bars = lower mobility distribution. HCD collision energy = 30. Concentration = 1 μ M equimolar in methanol.

Dual-gate = 1.0 ms width, 1.0 ms / step. Scans per step = 10. Orbitrap mass resolution setting = 140k.

For Table of Contents Only

